Arch. Metall. Mater. **67** (2022), 1, 181-187

DOI: https://doi.org/10.24425/amm.2022.137487

L. SOWA[1*], T. SKRZYPCZAK[1], P. KWIATOŃ[1]

NUMERICAL EVALUATION OF THE IMPACT OF RISER GEOMETRY ON THE SHRINKAGE DEFECTS FORMATION IN THE SOLIDIFYING CASTING

The work concerns of modeling the process of manufacturing machine parts by casting method. Making a casting without internal defects is a difficult task and usually requires numerous computer simulations and their experimental verification at the prototyping stage. Numerical simulations are then of priority importance in determining the appropriate parameters of the casting process and in selecting the shape of the riser for the casting fed with it. These actions are aimed at leading shrinkage defects to the riser, so that the casting remains free from this type of defects. Since shrinkage defects usually disqualify the casting from its further use, this type of research is still valid and requires further work. The paper presents the mathematical model and the results of numerical simulations of the casting solidification process obtained by using the Finite Element Method (FEM). A partial differential equation describing the course of thermal phenomena in the process of 3D casting creating was applied. This equation was supplemented with appropriate boundary and initial conditions that define the physical problem under consideration. In numerical simulations, by selecting the appropriate shape riser, an attempt was made to obtain a casting without internal defects, using a simple method of identifying their location. This is the main aim of the research as such defects in the casting disqualify it from use.

Keywords: Numerical simulations; solidification; casting defects; FEM

1. Introduction

The need to produce high-quality castings results in an intensive technological development of their production methods, which requires continuous research. These studies are mainly aimed at obtaining castings without internal defects of the high strength properties [1-3] or creating the layered castings that can work in high temperature conditions or be resistant to corrosion [4]. Research on real objects is difficult due to the high temperatures occurring there, which is why computer simulations make it possible to improve casting methods [1-2,5-12]. For the analysis of the casting process in three-dimensional space, an appropriate mathematical model should be formulated, taking into account only the most important phenomena occurring in the casting creation process. It is connected with the necessity to obtain an effective numerical solution, especially when we only have a general-purpose program while performing numerical simulations [7-9]. The complexity of the mathematical model is less important in the case of expensive programs mainly dedicated to foundry [1,2,5,6,11]. Some researchers neglect to take into account the movements of the liquid metal in the numerical analysis of the solidification process [7-9], because the movements have small values after filling the mould but, in turn, they focus on the analysis of the formation and growth of shrinkage cavity in the casting process [9]. This article analyses the solidification process of a casting using a model in which the movements of the molten metal were neglected. By comparing the obtained calculation results with the results presented in [11], obtained taking into account the movements of the liquid metal, their good agreement can be stated. The effectiveness of feeding the casting through the molten metal from the riser was checked using a cylindrical or conical riser. By observing the permanently changing shape of the solidus line, it was assessed whether it was closed in the area of the casting feed. Such a situation would mean no feeding of this area with liquid metal from the riser and the formation of shrinkage defects at this point of the casting. We try to avoid this situation by selecting the appropriate shape of the riser for the casting under consideration (conical or cylindrical), which was the aim of this work. At the same time, efforts were made to reduce the amount of metal needed to fill the mould cavity by using a cylindrical riser which, however, did not fulfil its role in feeding the casting.

[1] CZESTOCHOWA UNIVERSITY OF TECHNOLOGY, DEPARTMENT OF MECHANICS AND MACHINE DESIGN FUNDAMENTALS, DĄBROWSKIEGO 73, 42-200 CZĘSTOCHOWA, POLAND

* Corresponding Author E-mail: sowa@imipkm.pcz.pl

2. The mathematical description

The proposed model for numerical simulation of the casting solidification is based on the solution of the thermal conductivity equation in the form: [7-10]:

$$\rho c \frac{\partial T}{\partial t} = \nabla \cdot (\lambda \nabla T) + \rho_S L \frac{df_S(T)}{dt} \tag{1}$$

where: $T(\mathbf{x}, t)$ – the temperature [K], $\lambda(T)$ – the thermal conductivity coefficient [W/(m·K)], $\rho(T)$ – the density [kg/m^3], $c(T)$ – the specific heat [J/(kg·K)], L – the latent heat of solidification [J/kg], $f_s(T)$ – volume fraction of solid phase $f_s \in [0, 1]$, ρ_s – the density of solid phase [kg/m^3], t – time [s], $\mathbf{x}(x,y,z)$ – the coordinates of the vector of a considered node's position [m].

It was assumed that the solidification process of the metal occurs in a two-phase region, therefore the internal heat source is not visible in the heat conductivity equation, and the differential equation (1) takes the form [7-10]:

$$\nabla \cdot (\lambda \nabla T) - \rho C_{ef} \frac{\partial T}{\partial t} = 0 \tag{2}$$

In the solid-phase growth model used, the heat of phase change is introduced into effective specific heat [7]. Additionally, assuming a linear function of the solid phase fraction, the effective specific heat (C_{ef}) for each phase is determined as follows [7-9]:

$$C_{ef}(T) = \begin{cases} c_L(T), & T > T_L, \\ c_{LS}(T) + \dfrac{L}{T_L - T_S}, & T_S < T < T_L, \\ c_S(T), & T < T_S \end{cases} \tag{3}$$

where: T_S, T_L – the solidus and liquidus temperature of the analysed alloy [K], c_S, c_{LS}, c_L, – the specific heat of solid phase, mushy zone and liquid phase, respectively [J/(kg·K)].

The heat conductivity equation (2) was supplemented by appropriate initial and boundary conditions.

The initial conditions for the temperature fields were taken as [7-9]:

$$T(\mathbf{x}, t_0) = T_0(x, y, z) = \begin{cases} T_M & \text{on} \quad \Gamma_G \\ T_{in} & \text{in} \quad \Omega_L \\ T_M & \text{in} \quad \Omega_M \end{cases} \tag{4}$$

The boundary conditions in the considered task, assumed on the indicated surfaces (Fig. 1), were as follows [7-9]:

$$\begin{aligned} &\lambda_M \frac{\partial T_M}{\partial n}\Big|_{\Gamma_M} = -\alpha_M \left(T_M\Big|_{\Gamma_M} - T_a\right), \\ &\lambda_S \frac{\partial T_S}{\partial n}\Big|_{\Gamma_{G-}} = \lambda_G \frac{\partial T_G}{\partial n}\Big|_{\Gamma_{G-}}, \\ &\lambda_G \frac{\partial T_G}{\partial n}\Big|_{\Gamma_{G+}} = \lambda_M \frac{\partial T_M}{\partial n}\Big|_{\Gamma_{G+}}, \qquad \frac{\partial T}{\partial n}\Big|_{\Gamma_{1-1}} = 0 \end{aligned} \tag{5}$$

where: T_a – the ambient temperature [K], T_M, T_G – the temperature of mould and gap (protective coating), respectively [K],

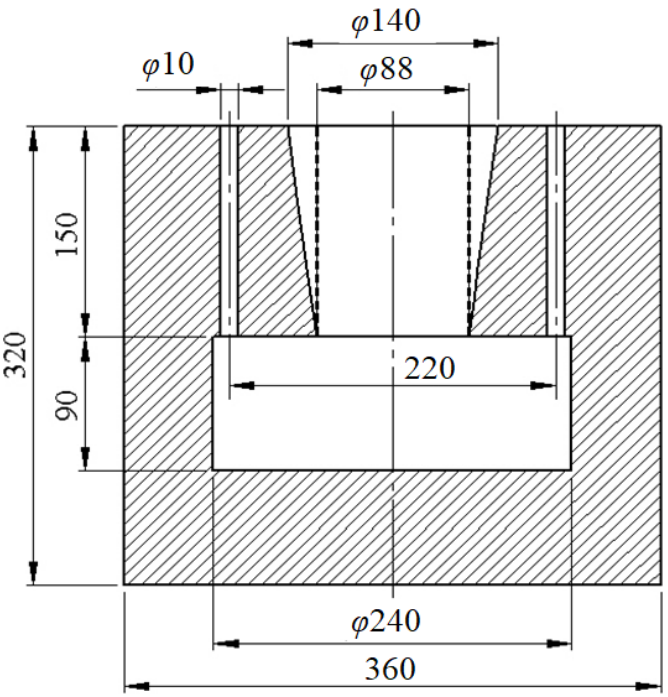

Fig. 1. A cross-section of the casting-mould system and identification of sub-regions of the region under consideration

λ_M, λ_G, λ_S – the thermal conductivity coefficient of mould, gap and solid phase, respectively [W/(m·K)], α_M – the heat-transfer coefficient between mould and ambient [W/(m^{2}K)], n – the outward unit normal surface vector [m].

In the numerical model, the finite element method was used in the weighted residuals formulate [7-10,12]. The equation (2) is multiplied by the weighting function (N) and integrated over the whole region (Ω), in this FEM formulation. As the result of using Galerkin's method, Ostrogradsky-Gauss-Green's theorem and the Euler's backward time integration scheme, the final following matrix equation global is obtained [7,9,10]:

$$(M_{KL} + K_{KL}) T_L^{s+1} = M_{KL} T_L^s + b_K^{s+1} \tag{6}$$

where the elements of individual matrixes define integrals:

$$\begin{aligned} K_{KL} &= \int_\Omega \lambda N_{,j}^K N_{,j}^L d\Omega, \\ M_{KL} &= \frac{1}{\Delta t} \int_\Omega \rho C_{ef} N^K N^L d\Omega, \\ b_K &= \int_\Gamma \lambda N^K T_{,j} n_j d\Gamma \end{aligned} \tag{7}$$

and these matrixes are called accordingly: K_{KL} is the global thermal conductivity matrix, M_{KL} – the global thermal capacity matrix, b_K – global vector associated with the thermal boundary conditions, T_L – vector of unknown nodal temperatures, s – time level.

Then, the Newton-Raphson iterative method was used to solve the matrix system of equations due to its quick convergence. By solving of matrix equation (6) is obtained the sought field of temperature in the considered area.

3. Numerical calculations

To analyse the impact of the riser shape on solidification of the casting, the following three-dimensional system of casting-mould was considered (Fig. 1). The mould is a cross section 360×320 and 360 mm in thickness and its internal surface is covered with a protective coating. This protective coating is made from a water suspension of quartzite dust with 2 mm thickness. In numerical calculations, the protective coating of the mould is modelled with an additional finite element placed between the areas of the casting and the mould with protective coating properties, which constitute a resistance to heat flow. The overall dimensions of the casting are equal to φ240×90 mm. Because, the computer calculations of the casting together with the conical or cylindrical riser are made, the dimensions of cylindrical riser amounts to φ88×150 mm and conical riser are equal φ88×φ140×150 mm. The numerical calculations were carried out for the casting made of low-carbon cast steel and the steel mould. The thermo-physical properties were taken from work [1,2,7] and are summarised in Table 1 for the casting and Table 2 for other regions under consideration.

TABLE 1

Material properties of the casting – cast steel

Material property	Solid phase ($T_M - T_S$)	Liquid phase ($T_L - T_{in}$)
ρ [kg/m^3]	7805 – 7800	7300 – 7295
c [J/(kg·K)]	640 – 644	830 – 834
λ [W/(m·K)]	48 – 45	23 – 21
Additional parameters		
T_L [K]	1810	
T_S [K]	1760	
L [J/kg]	270000	

The overheated metal with temperature T_{in} = 1850 K was poured into the steel mould with initial temperature T_M = 350 K. The heat-transfer coefficient (α) between the mould and ambient was equal α_M = 200 W/(m^{2}K) and on the upper surface of the riser between the slag and ambient α_s = 1 W/(m^{2}K) [5,7]. The ambient temperature (T_a) was equal to 300 K.

TABLE 2

Material properties used in the calculations for other regions

Material property	Mould	Protective coating
ρ [kg/m^3]	7200	1600
c [J/(kg·K)]	600	1670
λ [W/(m·K)]	42	0.3

The SolidWorks Simulation professional program was used for the calculations. A transient heat transfer analysis was performed only by conduction but with a phase change in the cooled metal, modelled by the temperature-dependent change in material properties in the non-solid phase of the solidifying region. The calculation process was carried out for the longitudinal-section shown in Fig. 1 on a 2.3 GHz IntelCore-i5 processor computer and it lasted approximately 7 hours. The geometry of the system under consideration was divided into 545 300 tetrahedral finite elements which are defined by 742 555 mesh nodes.

4. Discussion of the numerical simulations results

Many numerical simulations were performed to determine the influence of the riser shape on the process of obtaining a casting without shrinkage defects. The calculations were made for two riser shapes: conical (I variant) or cylindrical (II variant). The difference between variants I and II is only in the shape of the riser, the remaining casting parameters are the same in both variants. The possibility of reducing material consumption per riser was assessed, while maintaining its functionality for feeding the casting. Thermal phenomena occurring in the mould cavity from the moment of its complete filling (initial state Fig. 2) to the complete solidification of the casting were analysed (Figs 2-17).

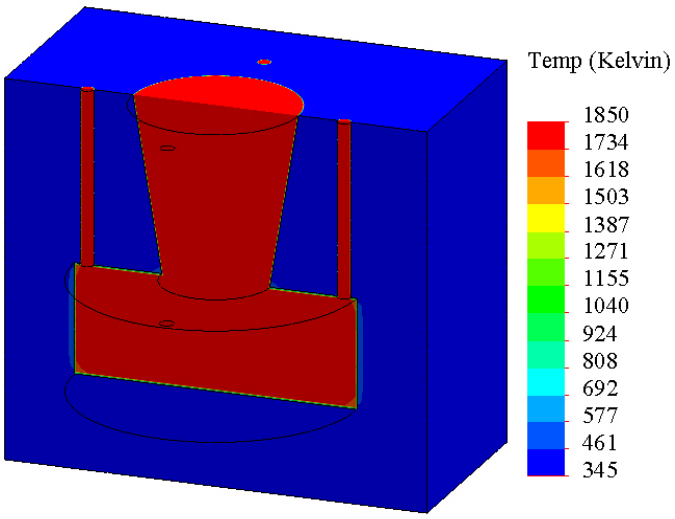

Fig. 2. Temperature distribution at t = 5 s, I variant

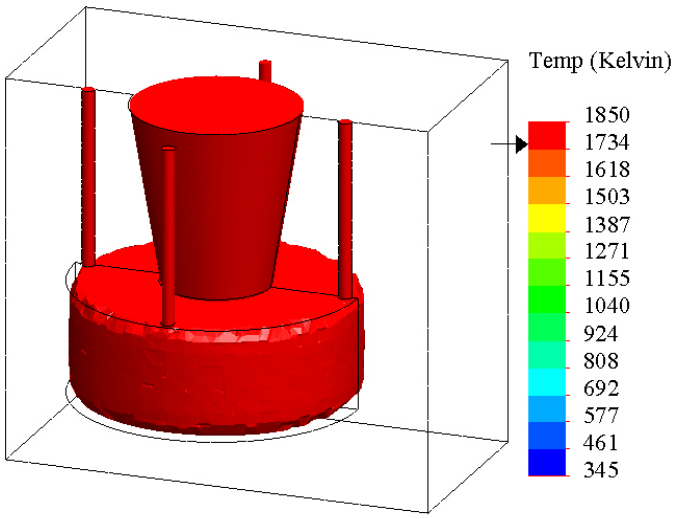

Fig. 3. Temperature field above the solidus temperature after 5 s, I variant

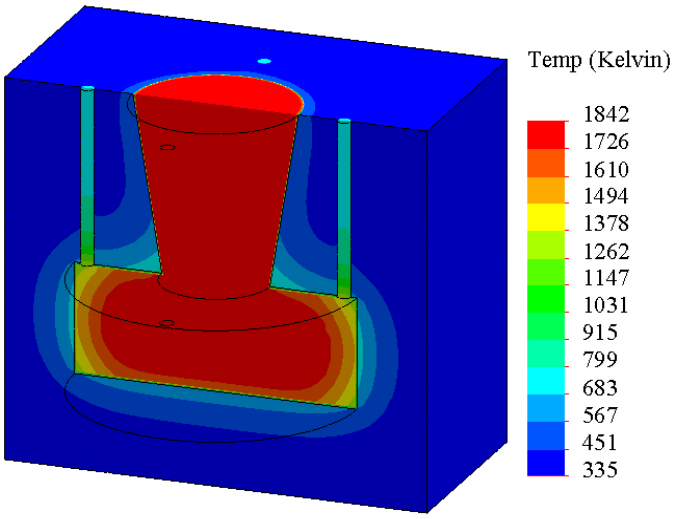

Fig. 4. Temperature distribution at t = 100 s, I variant

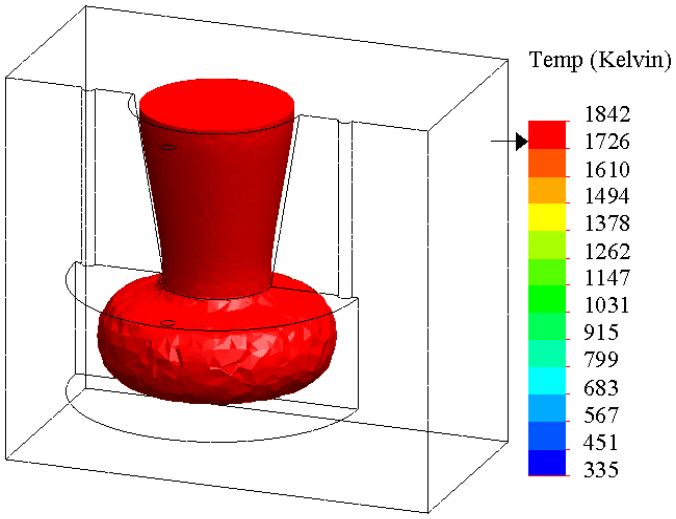

Fig. 5. Temperature field above the solidus temperature after 100 s, I variant

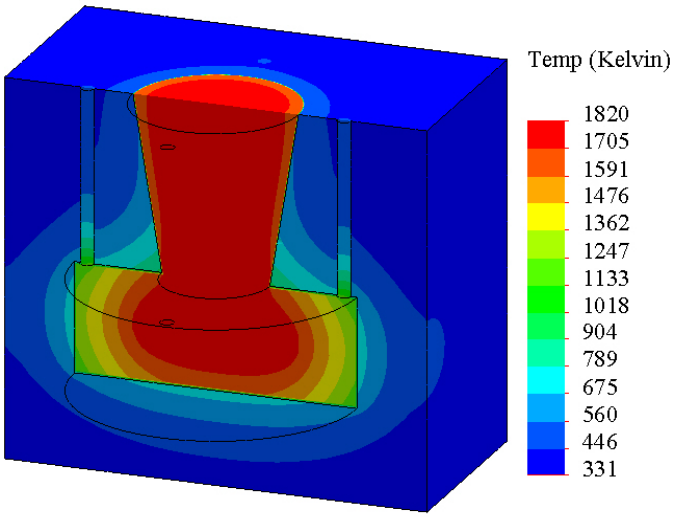

Fig. 6. Temperature distribution at t = 200 s, I variant

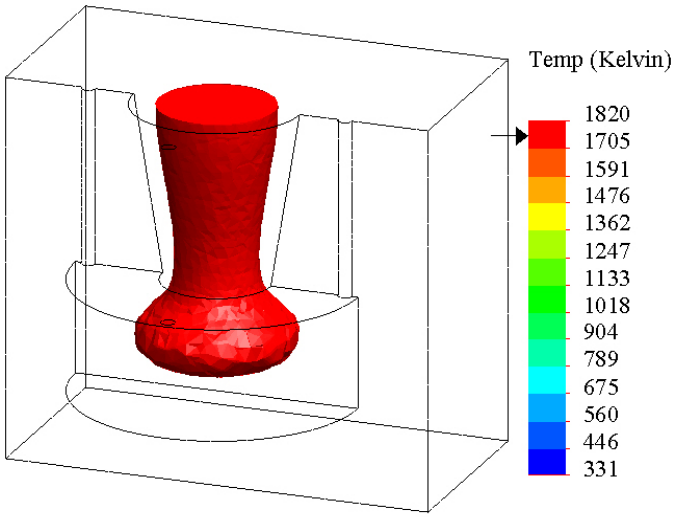

Fig. 7. Temperature field above the solidus temperature after 200 s, I variant

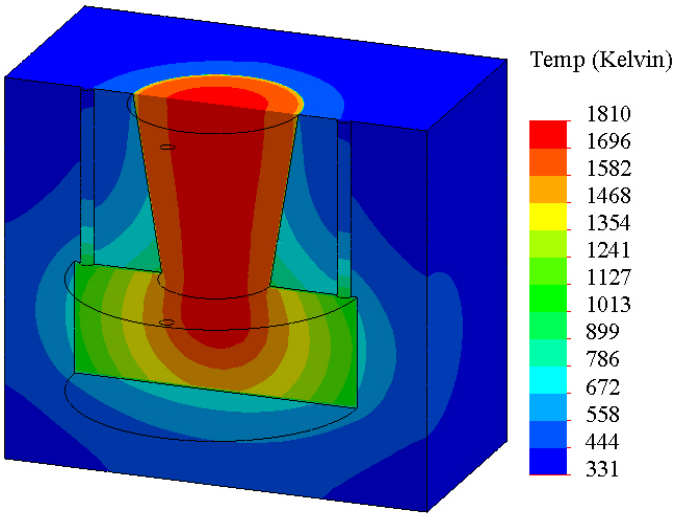

Fig. 8. Temperature distribution at t = 328 s, I variant

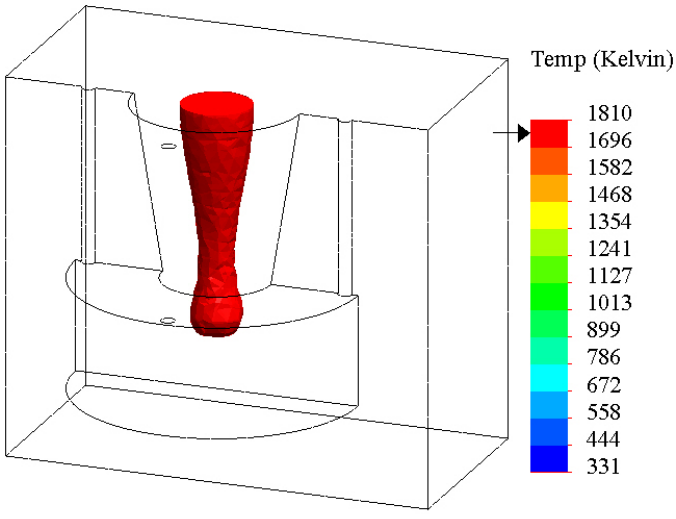

Fig. 9. Temperature field above the solidus temperature after 328 s, I variant

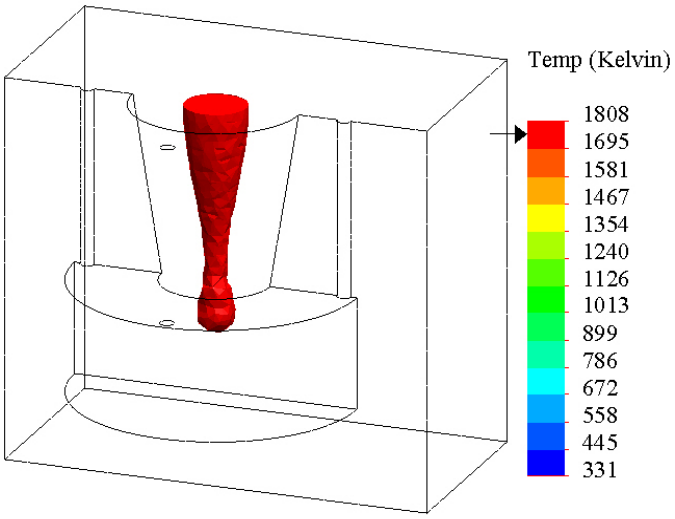

Fig. 10. Temperature field above the solidus temperature after 350 s, I variant

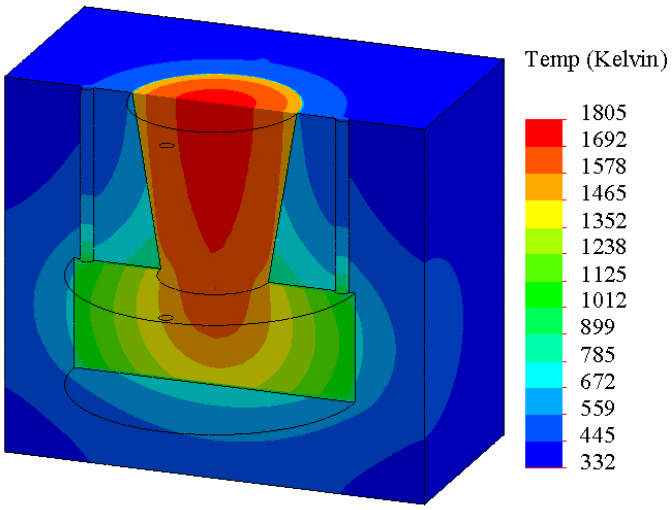

Fig. 11. Temperature distribution at t = 378 s, I variant

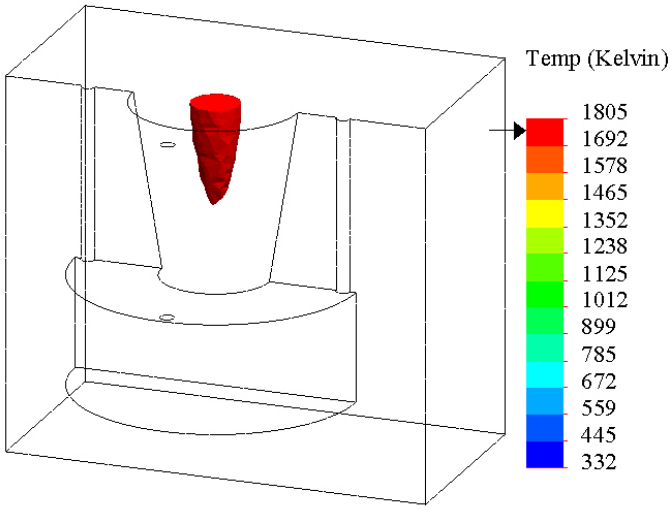

Fig. 12. Temperature field above the solidus temperature after 378 s, I variant

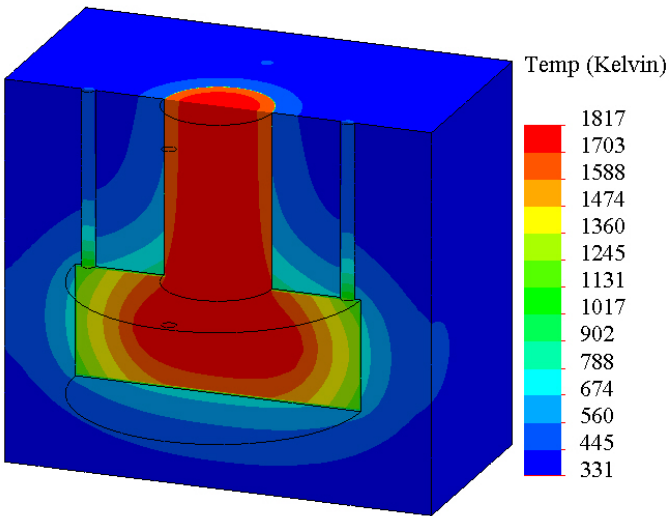

Fig. 13. Temperature distribution at t = 200 s, II variant

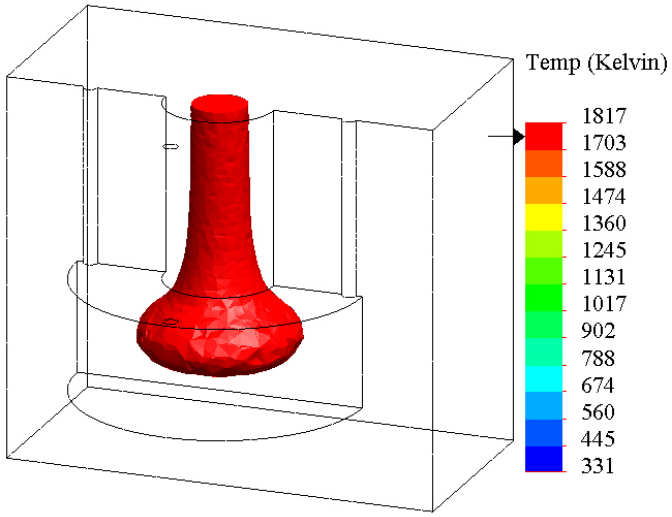

Fig. 14. Temperature field above the solidus temperature after 200 s, II variant

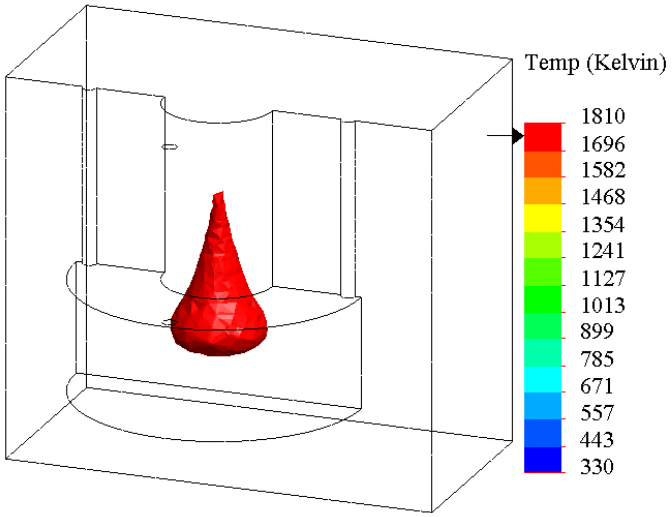

Fig. 15. Temperature field above the solidus temperature after 280 s, II variant

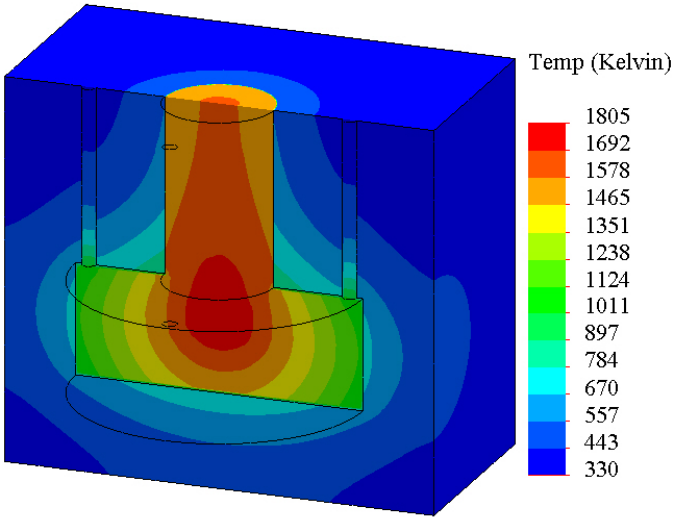

Fig. 16. Temperature distribution at t = 328 s, II variant

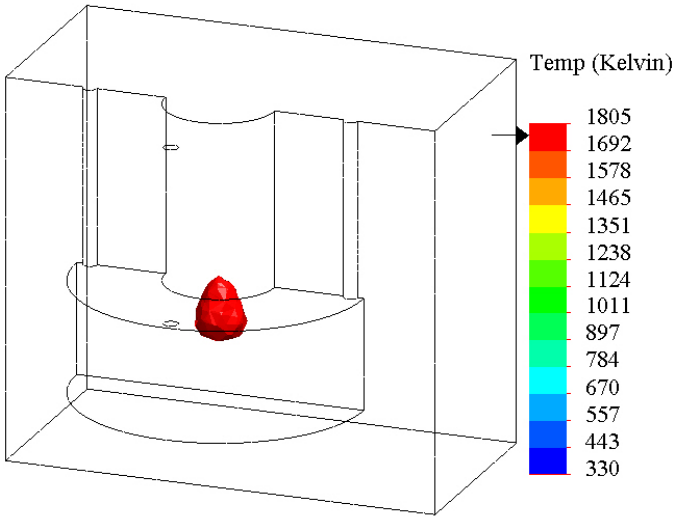

Fig. 17. Temperature field above the solidus temperature after 328 s, II variant

Examples of calculation results are shown in the form of temperature fields in Figs 2-12 for the casting together with the conical riser or in Figs 13-17 for the cylindrical riser. The temperature distribution figures show the temperature decrease in successive time steps in the whole considered casting-mould system in both variants. For a better identification of the volume of the non-solidified area, drawings of temperature fields are shown, in which only the temperature higher than the solidus temperature is visible. In subsequent time steps, this area is smaller and smaller until it indicates the place where the end of solidification of the metal occurs (Figs 11, 12, 16, 17). By observing the continuous moving of the solidus line during the directional solidification process of the molten metal, it is possible to obtain information about the formation of the casting without shrinkage defects. If this line moves fluently to the riser, where the solidification process of the considered system should end, the casting free of defects will be created (Fig. 12), if not, the defect will form in the casting (Fig. 17). We try to avoid the latter situation by selecting the appropriate shape and dimensions of the riser for the casting.

5. Conclusions

This paper focuses mainly on the computer simulation of the unsteady process of the cast steel solidification in a metal mould using the finite element method. Such an approach to the research of the casting solidification process is now quite often used due to the difficulties in conducting them in real objects, due to the high temperatures occurring there, the lack of visibility and the high cost of measuring devices. Moreover, numerical calculations allow for quick dimensional modification of the analysed casting system and for changing the conditions of the casting process, which is their great advantage at the stage of casting prototyping. The solidification process of the molten metal in the three-dimensional casting-riser-mould system was analysed, assessing whether the thermal conditions are conducive to the formation of shrinkage defects. Numerical calculations were made with the assumption of conical or cylindrical riser, obtaining temperature fields allowing follow the position of the solidus line in subsequent stages of the calculation (Figs 2-17). It was observed whether this line is not closing disconnecting the solidifying casting into smaller areas with a difficult supply to them of liquid metal from riser, because this would result in formation of shrinkage cavity in this place. Such a situation is not visible in the case of using the conical riser (Figs 11, 12). The end of solidification to occur in the upper part of the riser, which is allowed, because the riser with the shrinkage cavity created in this way is cut off and reprocessed. Changing the shape of the riser to cylindrical in order to reduce the material for the riser and reduce the production cost of the casting did not result in a good casting. In the final solidification period of the system casting-cylindrical riser, closing of the solidus line and location of the shrinkage cavity in the upper part of the casting was observed (Figs 16, 17), which proves that such the riser did not fulfil its task. Thus, the aim of this study was partially achieved, because the appropriate riser was selected to solidify the casting in a metal mould so that it was created without shrinkage defects, but the amount of material for the riser was not reduced, which requires further research. The next step in the scientific research of the casting solidification process would be to apply a mathematical model that takes into account the movements of the liquid metal, which will make it more complex, but nearer to reality. However, this will result in a significant extension of the computation time and problems with the stability of numerical computations in three-dimensional problems.

REFERENCES

[1] J. Hajkowski, P. Roquet, M. Khamashta, E. Codina, Z. Ignaszak, Arch. Foundry Eng. **17**, 57-66 (2017).
DOI: https://doi.org/10.1515/afe-2017-0011

[2] P.H. Huang, C.J. Lin, Int. J. Adv. Manuf. Technol. **79** (7), 997-1006 (2015). DOI: https://doi.org/10.1007/s00170-015-6897-5

[3] T. Tański, K. Labisz, B. Krupińska, M. Krupiński, M. Król, R. Maniara, W. Borek, J. Therm. Anal. Calorim. **123** (1), 63-74 (2016). DOI: https://doi.org/10.1007/s10973-015-4871-y

[4] J. Szajnar, T. Wróbel, A. Dulska, Journal of Casting & Materials Engineering **1** (1), 2-6 (2017). DOI: https://doi.org/doi.org/ 10.7494/jcme.2017.1.1.2

[5] S.L. Nimbulkar, R.S. Dalu, Perspectives in Science. **8**, 39-42 (2016). DOI: https://doi.org/10.1016/j.pisc.2016. 03.001

[6] P.H. Huang, J.K. Kuo, T.H. Fang, W. Wu, MATEC Web of Conferences. **185**, (2018). DOI: https://doi.org/10.1051/matecconf/ 201818500008

[7] L. Sowa, T. Skrzypczak, P. Kwiatoń, MATEC Web of Conferences. **254**, (2019). DOI: https://doi.org/10.1051/matecconf/ 201925402016

[8] A.S. Jabur, F.M. Kushnaw, J. Appl. Computat. Math. **6** (4), (2017). DOI: https://doi.org/10.4172/21689679.1000371.

[9] T. Skrzypczak, E. Węgrzyn-Skrzypczak, L. Sowa, Acta Physica Polonica A. **138** (2), 308-311 (2020). DOI: 10.12693/APhysPolA.138.308

[10] R.W. Lewis, E.W. Postek, Z. Han, D.T. Gethin, International Journal of Numerical Methods for Heat & Fluid Flow. **16** (5), 539-572 (2006). DOI: https://doi.org/10.1108/09615530610669102.

[11] I. Malik, A.A. Sani, A. Medi, J. Phys.: Conf. Ser. **1500**, (2020) DOI: https://doi.org/10.1088/1742-6596/1500/1/012036.

[12] M. Handrik, M. Vasko, P. Kopas, M. Saga, Communications **16** (3), 19-26 (2014). https://www.researchgate.net/publication/283112011